



# Experimental Investigations of Couette-Taylor-Poiseuille Flows Using the Electro-Diffusional Technique

Emna Berrich, Fethi Aloui, Jack Legrand

## ► To cite this version:

Emna Berrich, Fethi Aloui, Jack Legrand. Experimental Investigations of Couette-Taylor-Poiseuille Flows Using the Electro-Diffusional Technique. ASME 2016 Fluids Engineering Division Summer Meeting collocated with the ASME 2016 Heat Transfer Summer Conference and the ASME 2016 14th International Conference on Nanochannels, Microchannels, and Minichannels, Jul 2016, Washington, United States. 10.1115/FEDSM2016-7918 . hal-03439199

**HAL Id: hal-03439199**

**<https://uphf.hal.science/hal-03439199>**

Submitted on 7 Jul 2022

**HAL** is a multi-disciplinary open access archive for the deposit and dissemination of scientific research documents, whether they are published or not. The documents may come from teaching and research institutions in France or abroad, or from public or private research centers.

L'archive ouverte pluridisciplinaire **HAL**, est destinée au dépôt et à la diffusion de documents scientifiques de niveau recherche, publiés ou non, émanant des établissements d'enseignement et de recherche français ou étrangers, des laboratoires publics ou privés.



Distributed under a Creative Commons Attribution 4.0 International License

# EXPERIMENTAL INVESTIGATIONS OF COUETTE-TAYLOR-POISEUILLE FLOWS USING THE ELECTRO-DIFFUSIONAL TECHNIQUE

**Emna BERRICH**

Emna.berrich@univ-nantes.fr

LUNAM Université, GEPEA, CNRS,  
UMR6144, École des Mines de  
Nantes, DSEE  
4 rue Alfred Kastler - BP20722 44307  
Nantes Cedex 03 - France

**\* Fethi ALOUI**

\* Corresponding author:

Fethi.aloui@univ-valenciennes.fr

LAMIH UMR CNRS 8201, University  
of Valenciennes (UVHC)  
Department of Mechanical  
Engineering, Campus Le Mont Houy,  
F-59313 Valenciennes Cedex 9 –  
France

**Jack LEGRAND**

Jack.Legrand@univ-nantes.fr

LUNAM Université, Université de  
Nantes, CNRS, GEPEA, UMR6144,  
CRTT, 37 Boulevard de l'Université  
BP 406, 44602 Saint-Nazaire Cedex -  
France

## ABSTRACT

Couette-Taylor-Poiseuille flow CTPF consists on the superposition of Couette-Taylor flow to an axial flow. The CTPF flow hydrodynamics studies remain rather qualitative or numerical or are restricted to relatively low Taylor and/or axial Reynolds numbers. For more comprehensive and control of CTPF, especially for relatively high Taylor numbers and high axial Reynolds numbers, we investigated experimentally CTF with and without an axial flow, using the electro-diffusion ED method. This technique requires the use of Electro-Diffusion ED probe which allows the determination of the local mass transfer rate from the Limiting Diffusion current measurement delivered by the ED probe while it is polarized by a polarization voltage. From the local mass transfer (the Sherwood number), we determined the wall shear rate using different approaches. The results illustrate that low axial flow can generate a stabilizing effect on the CT flow. The time-evolutions of the local mass transfer and the wall shear rate are periodic. These evolutions characterize the waviness or the stretching of the vortices. However, Taylor Wavy Vortex Flow TWVF is destabilized under the effect of relatively important axial flow. The time-evolutions of wall shear rate are no longer periodic. Indeed, Taylor vortices are overlapped or completely destructed.

## NOMENCLATURE

A	Surface of the probe (m <sup>2</sup> )
C	Concentration (mol/m <sup>3</sup> )
D	Coefficient of diffusion (m <sup>2</sup> .s <sup>-1</sup> )

F	Frequency of oscillation (Hz)
g	Gap thickness between the front and the back segments (m)
h	Length of the gap between the rotating disk and the fixed one (m)
i	Current (A)
l	width of the probe (m)
P	Perimeter of the probe (m)
R	Radial distance (mm)
S	Wall shear stress (s <sup>-1</sup> )
t	Time (s)
v	Velocity (m.s <sup>-1</sup> )
X, Y	Coordinates (m)
Greek symbols	
β	Amplitude of the oscillation
ε	Constant used in the inverse method
θ	Directional angle relative to a pointer, fixed on the sandwich probe mantle (°)
Ω	Angular velocity of the rotating plate (rad.s <sup>-1</sup> )
ν	Kinetic viscosity (m <sup>2</sup> .s <sup>-1</sup> )
Superscripts	
*	Dimensionless
–	Temporal average
Subscripts	
exp	Experimental
num	Numerical
grad	Gradient
Pe	Peclet number
Re	Reynolds number
Sh	Sherwood number

## INTRODUCTION

The Couette-Taylor Poiseuille CTP flow consists on the superposition of an axial flow to Couette-Taylor flow. An axial flow can have a stabilizing effect for Taylor Vortex Flow TVF [1]. It can delay the appearance of the first instability to TVF mode. However, an axial flow can also have a stabilizing effect on TVF flow for specific range of  $Re$  ( $0 < Re_{ax} < 15$ ) but not another range ( $15 < Re < 25$ ) [2]. In this paper, we present an experimental investigation using the Electro-Diffusion method to study CTP flows taking into account the history effect, for relatively large Taylor numbers and axial Reynolds numbers ( $Ta < 181.81$ ) and ( $Re_{ax} < 52.75$ ).

## EXPERIMENTAL APPARATUS AND ELECTRO-DIFFUSION METHOD

The experimental installation of Couette-Taylor-Poiseuille is presented on Figure 1. It contains two coaxial cylinders, a rotating inner one and a fixed outer one. The radius of respectively the inner cylinder and the outer one are  $R_1 = 85.5 \text{ mm} \pm 0.2$  and  $R_2 = 100 \text{ mm} \pm 0.2$ . The height is equal to  $H = 450 \text{ mm} \pm 0.5$ . The radius ratio is thus  $\eta = 0.855$ . The aspect ratio is  $\Gamma = 31$ . The system is constituted also by a storage tank, a pump; a by-pass; a flowrate control valve, a flowmeter; a CT feeder tank; a drain valve; and an electrical motor which assure the inner cylinder motion.

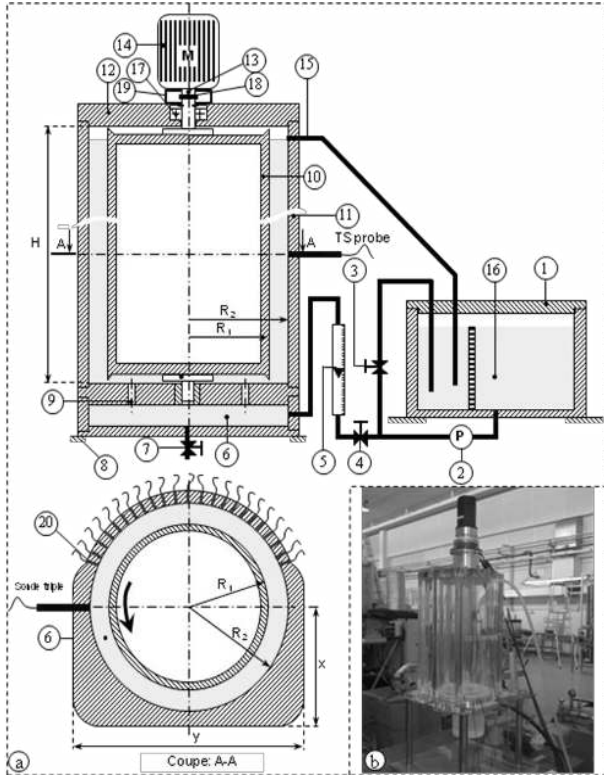


Figure 1. Experimental installation

A ferri-ferrocyanure of potassium is used as electrochemical solution. Its concentration is equal to  $25 \text{ mol/m}^3$ . An access of

the sulfate of potassium  $K_2SO_4$  ( $130 \text{ mol/m}^3$ ) is used as supporting electrolyte. A dispersion of 2.5% of Kalliroscope particles is added to visualize the flow.

The 39 electrochemical sensors (38 Single probes and triple probe) must be flush with the internal wall of the outer cylinder end to ensure the polarographic study of vortex-wall interaction. Bonding and securing operations simple probes is relatively difficult due to the cylindrical geometry of the experimental device. Two neighboring sensors are spaced apart by an angle of 7 degrees on the circumference of the inner wall of the outer cylinder of the SCT (Figure2). The two horizontal rows are spaced by a distance of 10 mm. 14 single probes are arranged on a vertical row. A single pair of probes disposed vertically are spaced 10 mm. Two neighboring pairs of single probes are arranged vertically spaced 54 mm.

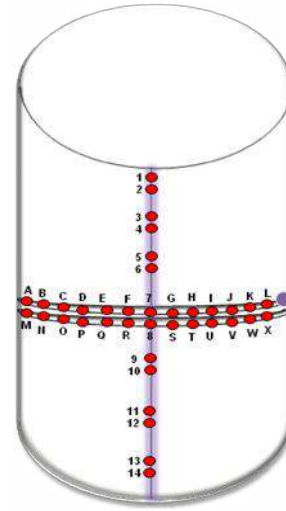


Figure 2. Electrochemical probes DISPOSITION FROM 1 to 14 and from A to X

## RESULTS AND DISCUSSION

The Taylor number characterizes the instabilities apparition. It can be written as:

$$Ta = \frac{\tau_v}{\tau_{cent}} = \frac{\Omega R_{int} \delta}{\nu} \sqrt{\frac{\delta}{R_{int}}} = Re_i \sqrt{\frac{\delta}{R_{int}}} \quad (1)$$

Where the azimuthal Reynolds number is defined by:

$$Re = \frac{\tau_v}{\tau_a} = \frac{\Omega R \delta}{\nu} \quad (2)$$

### 1. Effect of axial flow on mass transfer evolution

#### 1.1. Indirect protocol

We defined an experimental protocol to study the protocol history effect on the hydrodynamic CTPF flows behaviour: we firstly impose an ascendant axial flow to the fluid at rest on the CTS gap. When the regime is established, we superposed the azimuthal flow. We named this protocol "the indirect protocol".

The axial Reynolds number is defined as:

$$Re_{ax} = \frac{u_{ax} \cdot d}{\nu} \quad (5)$$

Where  $u_{ax}$  is the axial velocity imposed to the Taylor Vortex flow and  $\nu$  is the kinematic viscosity.

We firstly present a case of low axial flow without any azimuthal motion. The mass transfer time evolution is presented in Figure 3 for  $Re_{ax} = 2.64$ . As we can see, the Sherwood numbers values are positive for all the axial and horizontal coordinates (probes positions).

The time evolution of mass transfer for low ( $Re_{ax} = 1$  and  $Ta = 45.45$ ), ( $Re_{ax} = 2.64$  and  $Ta = 90.90$ ) and relatively high  $Re_{ax}$  ( $Re_{ax} = 20.76$  and  $Ta = 181.81$ ) are respectively presented in Figure 4 to 6.

$Ta = 45.45$  corresponds to the apparition of the first instability. The visualization using Kalliroscope [3] illustrates that at low axial flow ( $Re_{ax} = 0.94$ ), the Taylor vortices start to move in the axial flow direction. At  $Re_{ax} = 1.45$ , helical modes with an increasing number of helices which have a “helicity” opposite to the imposed axial flow are developed. The helical vortices celerity varies between 1 to 1.3 times the axial flow rates. This confirms the results of [4].

When the axial Reynolds number increases, the mass transfer becomes having sinusoidal evolution. This variation characterize vortices apparition. It increases when the Taylor number increases. For a same proportional forces effect (axial/azimuthal), the Sherwood number becomes more important when the axial Reynolds number increases.

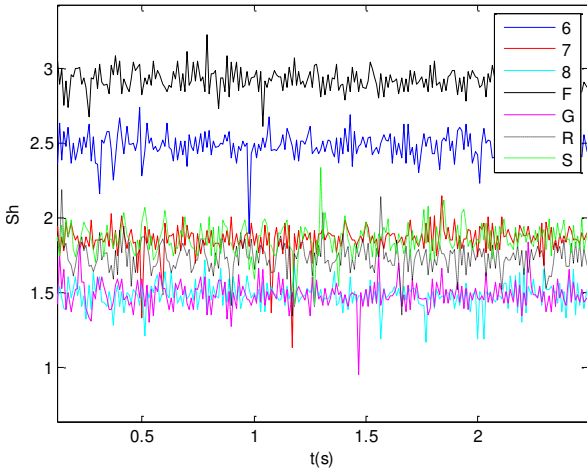


Figure 3. Time evolution of the Sherwood number for  $Re_{ax} = 2.64$

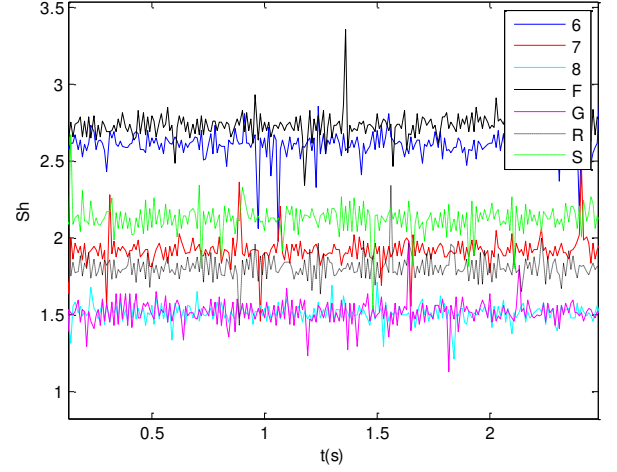


Figure 4. Time evolution of the Sherwood number for  $Re_{ax} = 1$  and  $Ta = 45.45$

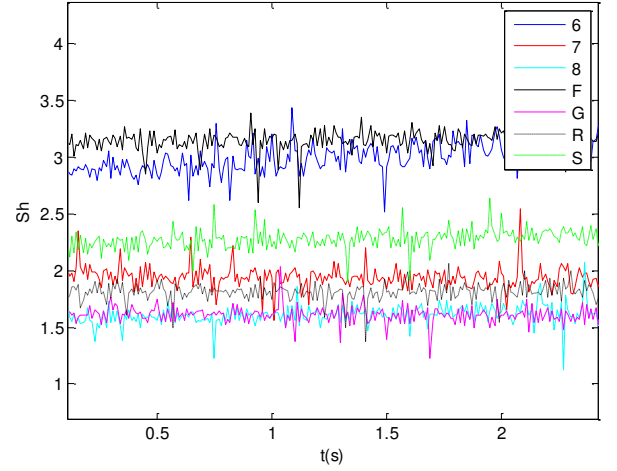


Figure 5. Time evolution of the Sherwood number for  $Re_{ax} = 2.64$  and  $Ta = 90.90$

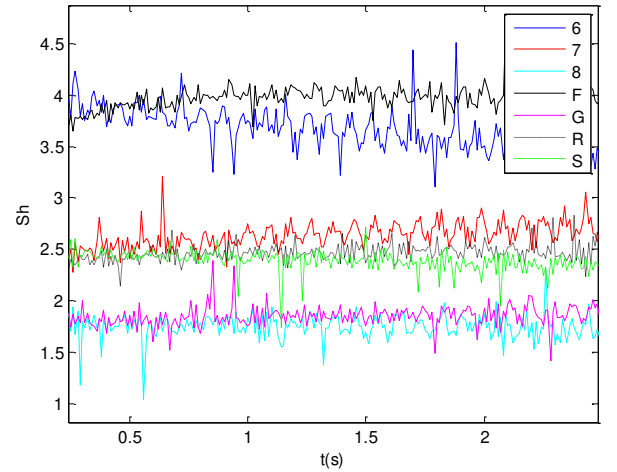


Figure 6. Time evolution of the Sherwood number for  $Re_{ax} = 20.76$  and  $Ta = 181.81$

## 1.2. Direct protocol

We initially impose an azimuthal motion to the fluid at rest. When the regime is established, we superposed the axial flow. We named this protocol “the direct protocol”.

The time evolution of the Sherwood number for relatively low axial Reynolds numbers at the first instability ( $Ta = 45.45$  and  $Re_{ax} = 0.94$ ), ( $Ta = 181.81$  and  $Re_{ax} = 1.10$ ), and high Reynolds number ( $Ta = 181.81$  and  $Re_{ax} = 52.75$ ). As we can see, the vortices manifest their presence by the mass transfer variation.

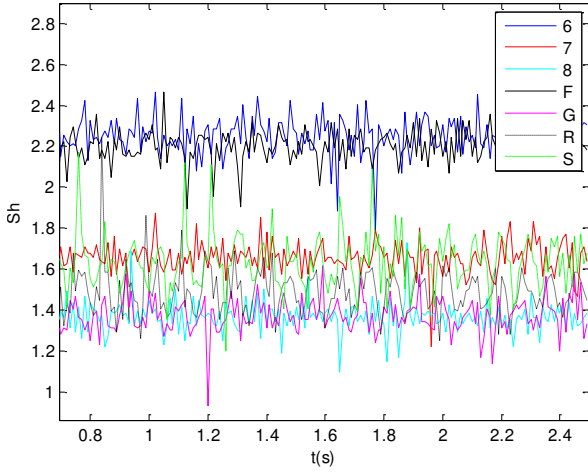


Figure 7. Time evolution of the Sherwood number for  $Ta = 45.45$  and  $Re_{ax} = 0.94$

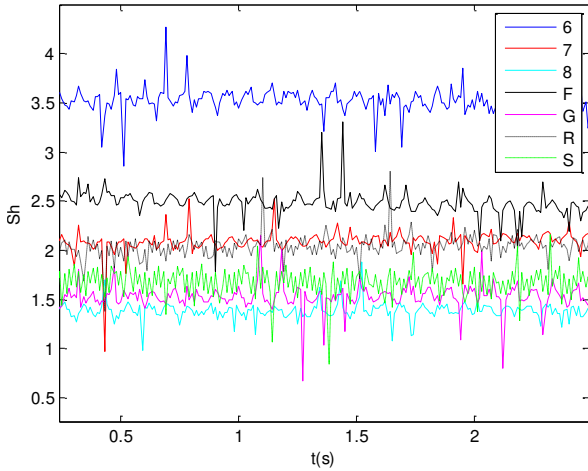


Figure 8. Time evolution of the Sherwood number for  $Ta = 181.81$  and  $Re_{ax} = 1.10$

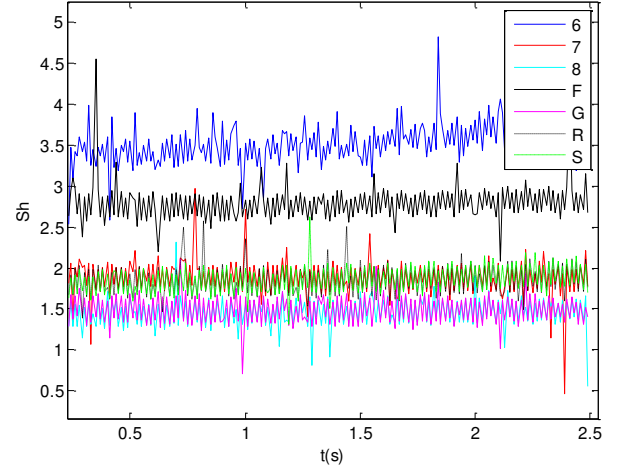


Figure 9. Time evolution of the Sherwood number for  $Ta = 181.81$  and  $Re_{ax} = 52.75$

## 2. Axial flow effect on wall shear rate evolution

### 2.1. Direct protocol

#### 2.1.1. Low axial flow

The wall shear rate evolution is determined from the mass transfer rate, using respectively Leveque solution, Sobolik et al., solution and Deslouis solution. These methods are well developed on our previous publication [5] and other works [6]. The wall shear rate evolution is presented for low Reynolds numbers without an azimuthal flow ( $Re_{ax} = 2.64$ ) respectively in Figure 10-12. As we can see, the vortices manifest themselves by the presence of wall shear rate variations. However, the Leveque solution shear rate remains always positive. While, Sobolik et al., and Deslouis solutions allow obtaining negative and positive rate values characterizing the presence of reversing flow.

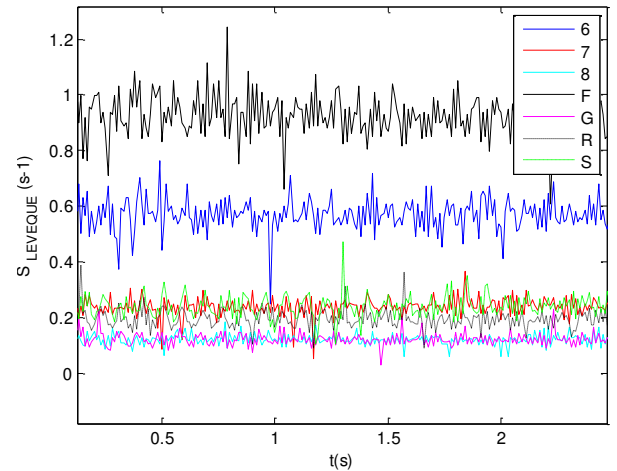


Figure 10. Time evolution of wall shear rate (Leveque method) for  $Re_{ax} = 2.64$

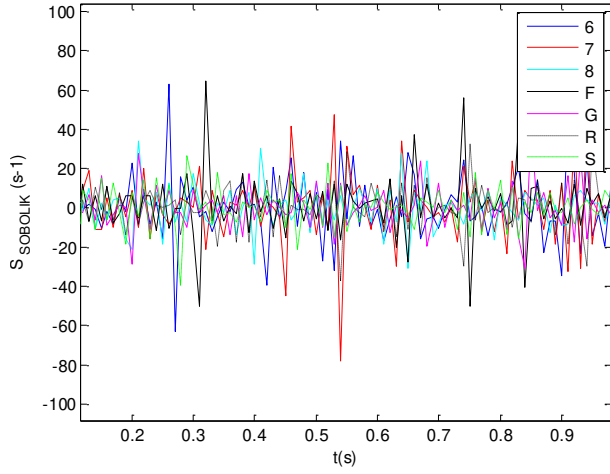


Figure 11. Time evolution of wall shear rate (Sobolik et al. method) for  $Re_{ax} = 2.64$

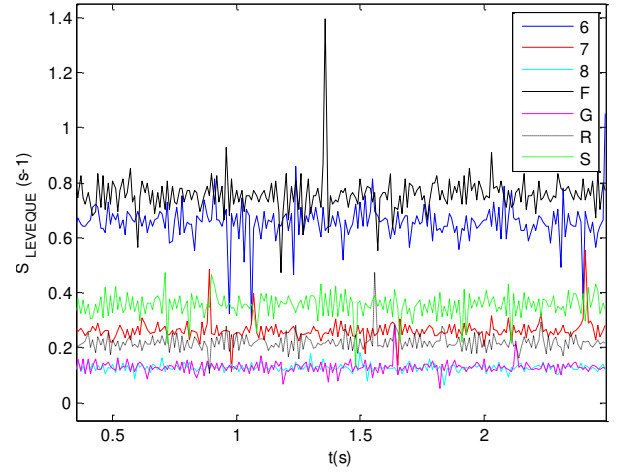


Figure 13. Time evolution of wall shear rate (Leveque method) for  $Re_{ax} = 1$  and  $Ta = 45.45$

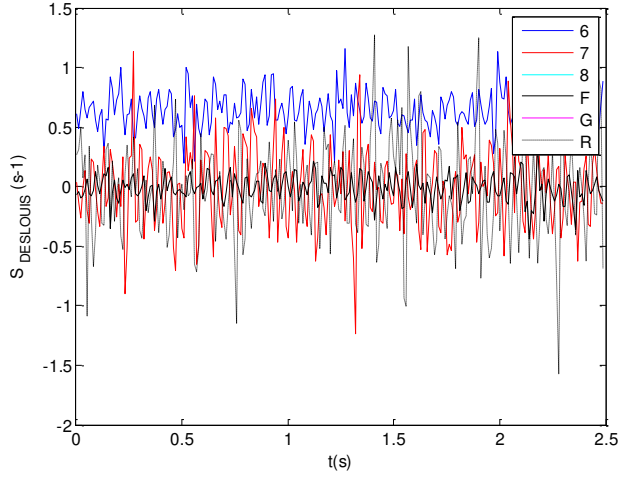


Figure 12. Time evolution of wall shear rate (Delouis et al. method) for  $Re_{ax} = 2.64$

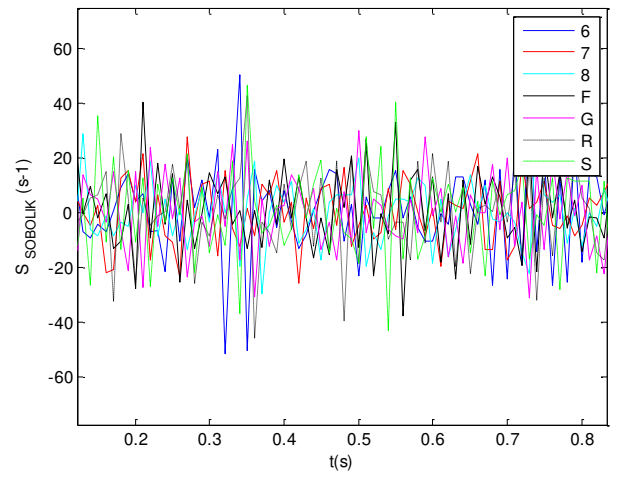


Figure 14. Time evolution of wall shear rate (Sobolik et al. method) for  $Re_{ax} = 1$  and  $Ta = 45.45$

### 2.1.2. Low axial flow effect on CF instability

The wall shear rate evolution is illustrated for low Reynolds numbers with an azimuthal flow ( $Re_{ax} = 1$  and  $Ta = 45.45$ ), respectively in Figure 13-15. In spite of a well developed axial flow, the vortices appear.

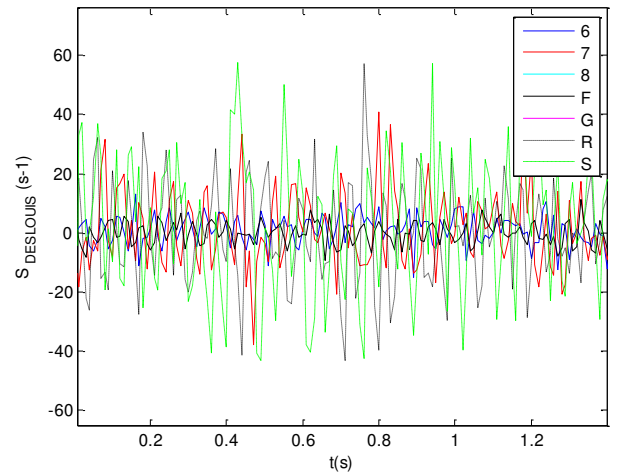


Figure 15. Time evolution of wall shear rate (Delouis et al. method) for  $Re_{ax} = 1$  and  $Ta = 45.45$



### 2.1.3. Low axial flow effect on WTVF

The wall shear rate evolution is presented for low Reynolds numbers with an azimuthal flow:  $Re_{ax} = 2.64$  and  $Ta = 90.90$ , respectively in Figure 16-18. The vortices appear when we initially impose an axial Reynolds corresponding to  $Re_{ax} = 2.64$ . Leveque solution shear rate remains always positive. It is attenuated comparing to Sobolik et al., and Deslouis solutions.

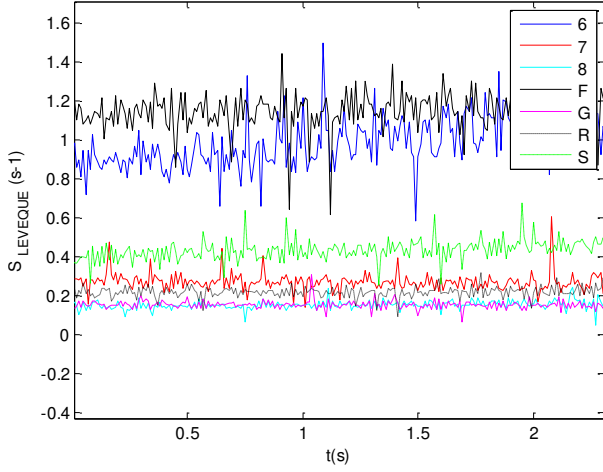


Figure 16. Time evolution of wall shear rate (Leveque method) for  $Re_{ax} = 2.64$  and  $Ta = 90.90$

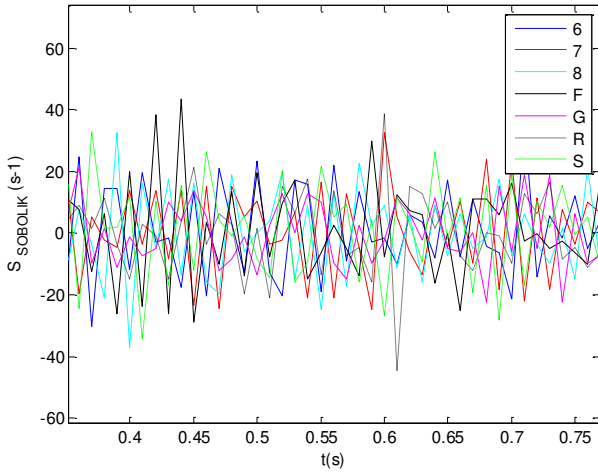


Figure 17. Time evolution of wall shear rate (Sobolik et al. method) for  $Re_{ax} = 2.64$  and  $Ta = 90.90$

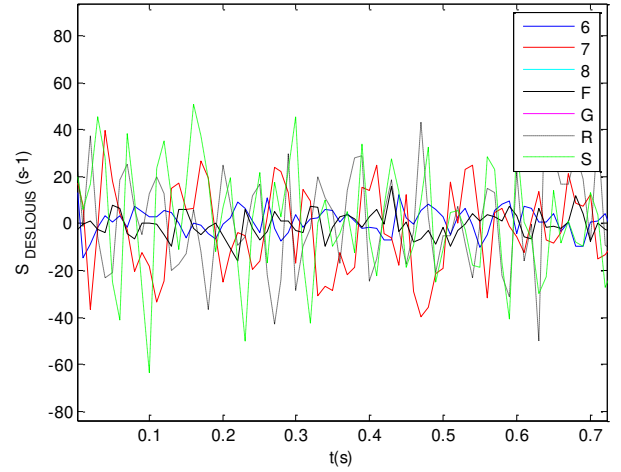


Figure 18. Time evolution of wall shear rate (Deslouis et al. method) for  $Re_{ax} = 2.64$  and  $Ta = 90.90$

### 2.1.4. High axial flow effect on WTVF

The wall shear rate evolution is illustrated for relatively high Reynolds numbers with an azimuthal flow:  $Re_{ax} = 20.76$  and  $Ta = 181.81$  respectively in Figure 19-21. The vortices appear even if an axial flow corresponding to  $Re_{ax} = 20.76$  is well developed. The shear rate depends on the special disposition of the probes.

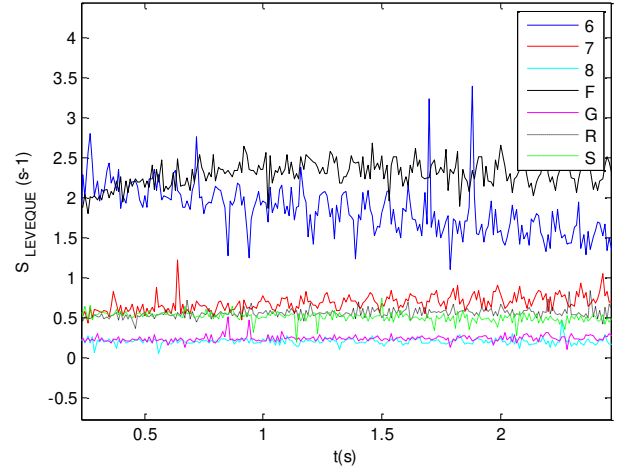


Figure 19. Time evolution of wall shear rate (Leveque method) for  $Re_{ax} = 20.76$  and  $Ta = 181.81$

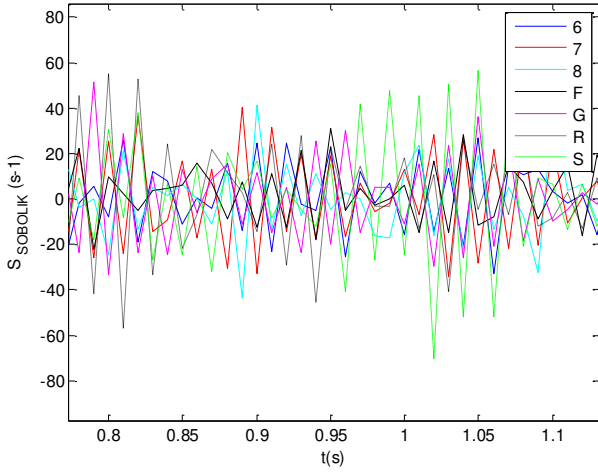


Figure 20. Time evolution of wall shear rate (Sobolik et al. method) for  $Re_{ax} = 20.76$  and  $Ta = 181.81$

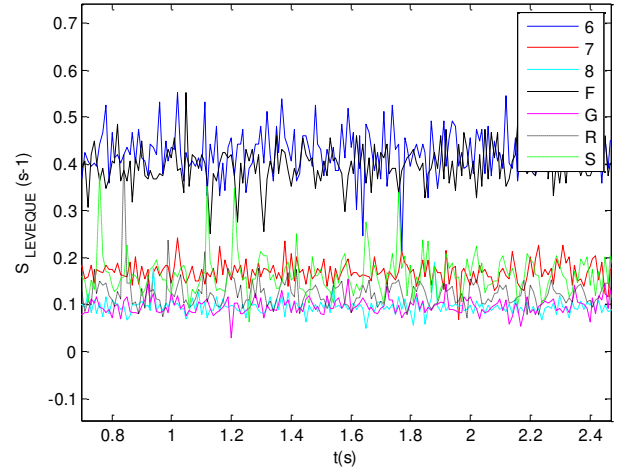


Figure 22. Time evolution of wall shear rate (Leveque method) for  $Ta = 45.45$  and  $Re_{ax} = 0.94$

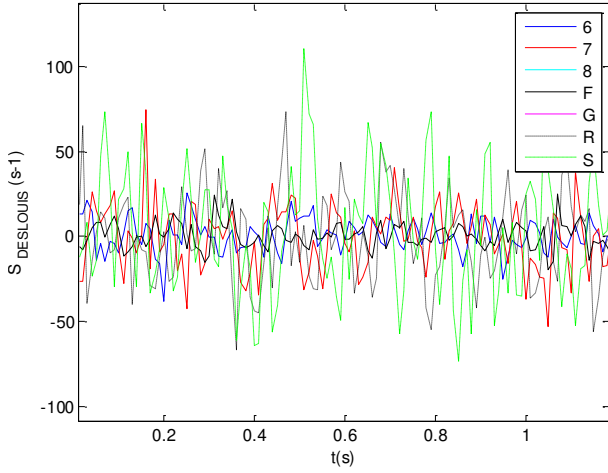


Figure 21. Time evolution of wall shear rate (Deslouis et al. method) for  $Re_{ax} = 20.76$  and  $Ta = 181.81$

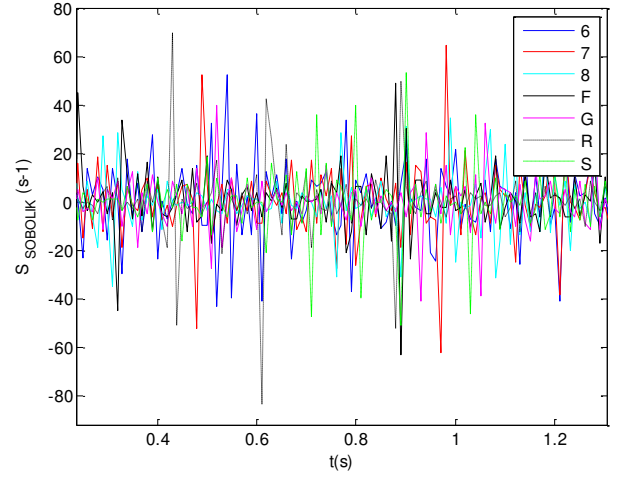


Figure 23. Time evolution of wall shear rate (Sobolik et al. method) for  $Ta = 45.45$  and  $Re_{ax} = 0.94$

## 2.2. Indirect protocol

### 2.2.1. Low axial flow effect on CT instability

The wall shear rate evolution is presented for  $Ta = 45.45$  and  $Re_{ax} = 0.94$  in Figure 22-24. The wall shear rate values are lower than the indirect protocol case.

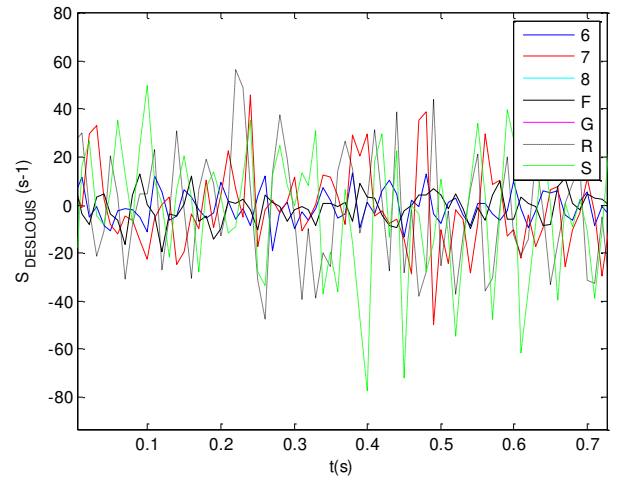


Figure 24. Time evolution of wall shear rate (Deslouis et al. method) for  $Ta = 45.45$  and  $Re_{ax} = 0.94$



### 2.2.2. Low axial flow effect on WVF

The wall shear rate evolution is presented for  $Ta = 181.81$  and  $Re_{ax} = 1.10$  in Figure 25-27. The wall shear rate increases when we increase the Taylor number for a same axial Reynolds number. It has a quasi-sinusoidal evolution characterizing that the vortices persists.

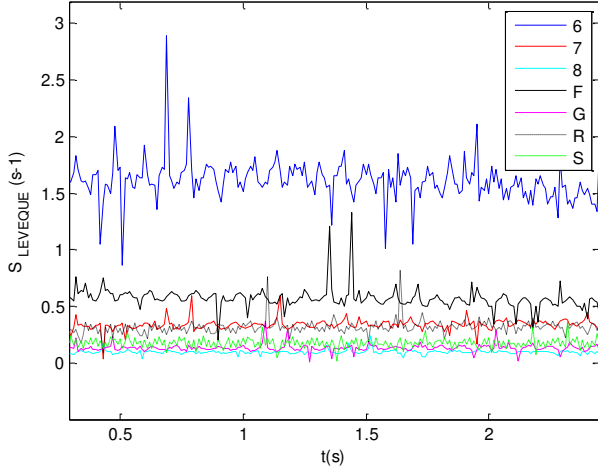


Figure 25. Time evolution of wall shear rate (Leveque method) for  $Ta = 181.81$  and  $Re_{ax} = 1.10$

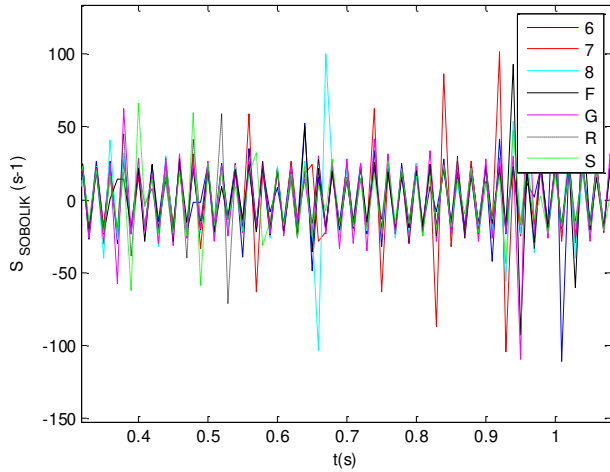


Figure 26. Time evolution of wall shear rate (Sobolik et al. method) for  $Ta = 181.81$  and  $Re_{ax} = 1.10$

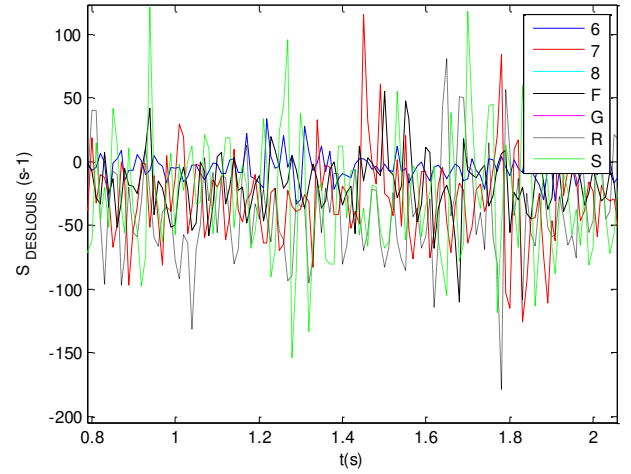


Figure 27. Time evolution of wall shear rate (Deslouis et al. method) for  $Ta = 181.81$  and  $Re_{ax} = 1.10$

### 2.2.3. High axial flow effect on WVF

The wall shear rate evolution is presented for  $Ta = 181.81$  and  $Re_{ax} = 52.75$  in Figure 28-30. Comparing to low Reynolds number case, the wall shear rate decreases when we increase the axial Reynolds number. There is vortices detachment.

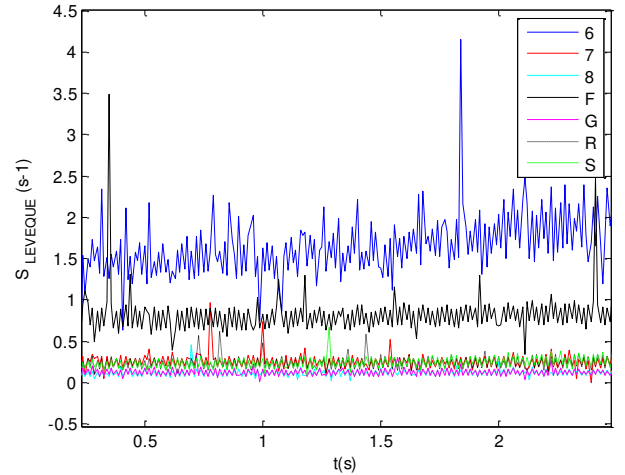


Figure 28. Time evolution of wall shear rate (Leveque method) for  $Ta = 181.81$  and  $Re_{ax} = 52.75$

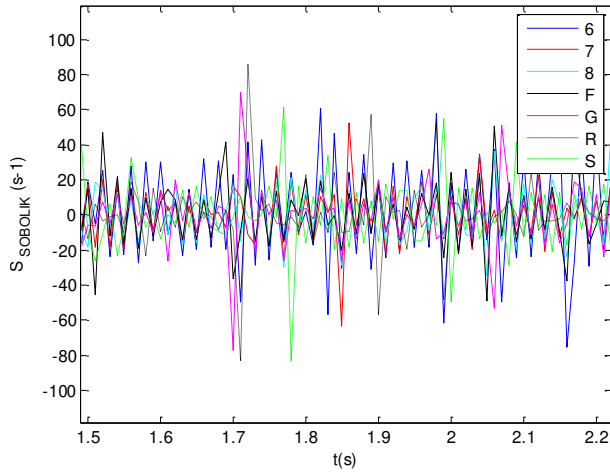


Figure 29. Time evolution of wall shear rate (Sobolik et al. method) for  $Ta = 181.81$  and  $Re_{ax} = 52.75$

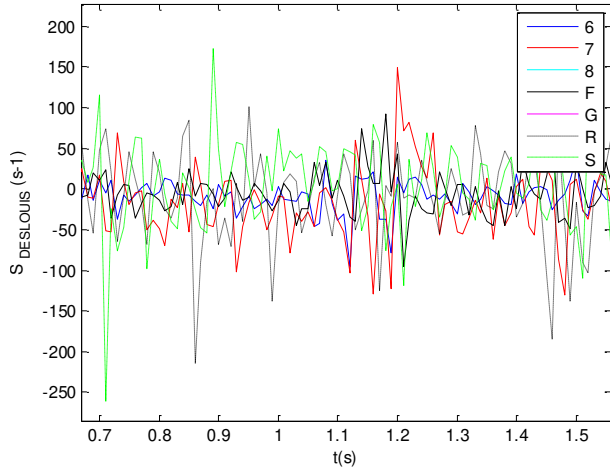


Figure 30. Time evolution of wall shear rate (Deslouis et al. method) for  $Ta = 181.81$  and  $Re_{ax} = 52.75$

## CONCLUSION

Mass transfer and wall shear rate time evolution for different horizontal and vertical CTPF positions, according to direct and indirect protocol are presented. The history effect are illustrated for relatively large range of Taylor and axial Reynolds numbers. Axial flow have a stabilizing effect on vortices or a destabilizing effect according to the torsional flow ( $Ta$ ) and axial flow ( $Re$ ) ratio. In such destabilizing cases, the vortices are either folded or stretched or overlapped or completely destructed. In other cases, it persists.

## ACKNOWLEDGMENTS

This work was supported by the laboratories GEPEA UMR CNRS 6144 (University of Nantes), LAMIH (UMR CNRS 8201 (University of Valenciennes) and the “Agence Nationale de la Recherche (ANR), France”, by the grant n° ANR-08-BLAN-0184-02. These supports are gratefully acknowledged.

## REFERENCES

- [1] Cornish, J. A., 1933, “Flow of water through fine clearances with relative motion of the boundaries”, *Proc. R. Soc. Lond.* Vol. 140, 227-240.
- [3] Berrich, E., Aloui, F., Legrand, J., 2012. “On the stability of Taylor - Couette Flow with Axial Flow”, *Proceedings of the ASME2012 Fluids Engineering Division Summer Meeting, And 7th Symposium on Flow Manipulation and Active Control*, July 8-12, 2012, Puerto Rico, USA, FEDSM2012-72235
- [4] Johnson E. C., Lueptow R. M., 1997, “Hydrodynamic stability of flow between rotating porous cylinders with radial and axial flow”, *Phys. Fluids*, Vol. 9, 3687.
- [5] Berrich, E., Aloui, F., Legrand, J., 2012. “Synchronization between PIV and Electro-diffusion techniques for the characterization of Wavy Taylor Vortex flows with axial flows”. *Turbulence, Heat and Mass Transfer* 7, 2012, DOI: 10.1615/ICHMT. ProcSevIntSymp TurbHeatTransf Pal.590.
- [6] Kristiawan, M., Tomas, Jirout T., El Faye, A., Sobolik, V., 2011. “Wall shear rate components for wavy Taylor-Couette flow”. *Experimental Thermal and Fluid Science* 35, pp. 1304–1312.